SVD H^{∞} Controller Design for an Active Horizontal Spray Boom Suspension.

Jan Anthonis[†], Herman Ramon
Department of Agro-Engineering and Economics
Laboratory of Agricultural Machinery and Processing
K.U.Leuven, Kardinaal Mercierlaan 92, 3001 Heverlee, BELGIUM

Abstract

An active suspension, acting as a band stop filter, to reduce the horizontal motions of an agricultural spray boom, is designed. Because the translational and the rotational behaviour of the system can be separated, a super optimal SVD H^{∞} controller is achieved by two single SISO designs. Black box frequency domain identification methods render continuous models. Accelerometer drift, performance and robustness issues are tackled. The final active horizontal suspension is validated on a commercial available spray boom.

1 Introduction

In agriculture, application of pesticides and herbicides by means of a spray boom is one of the most important field operations. Spray booms are large, weakly damped elastic structures with a working width up to 40 m. Field undulations, transmitted through the tractor, excite the boom and give rise to large spray boom motions in the horizontal and the vertical plane. Measurements (Speelman and Jansen, 1974) and simulations with experimental (Langenakens *et al.*, 1995) and analytical (Ramon and De Baerdemaeker, 1997) models have demonstrated that undesired horizontal spray boom vibrations are one of the main causes of an uneven spray deposit distribution and are at least as important as rolling of the boom. To supply each plant with a sufficient dose, farmers spray systematically too much, resulting in ecological damage and economical loss.

The study of the horizontal behaviour of spray booms has been initiated by (Ramon, 1993). To investigate the possibilities of an active horizontal suspension, a controller based on the LQG-LTR design strategy has been implemented successfully on a flexible beam, having eigenfrequencies comparable with common available spray booms (Ramon, 1993), (Ramon and De Baerdemaeker, 1996). One end of the boom in the form of an at one end clamped flexible beam has been considered and the flexible deformations, measured by a displacement sensor, induced by translational accelerations have been controlled. In this paper, a horizontal active suspension is designed for a small sized commercial available spray boom. Contrary to the previous work, two degrees of freedom are controlled : translational vibrations in the driving direction (jolting) and rotations around a vertical axis perpendicular to the horizontal plane (yawing). Vibrations, measured by accelerometers, due to flexibility's of the structure and rigid body modes as well are attenuated.

[†] Email: *jan.anthonis@agr.kuleuven.ac.be*

First a description of the experimental arrangement is given. Peculiar properties with respect to eigenvalues and singular values of the system, important for subsequent model identification and controller design are discussed in a next section. Continuous models are deduced by applying black box frequency domain identification algorithms. The design of an H^{∞} controller, trading of between robustness and performance and avoiding drift propagation to the output, is tackled in a next section. Finally, the controller is implemented on the test stand, performance and robustness are investigated and conclusions are drawn.

2 Description of the experimental arrangement

The experimental arrangement and a clarifying sketch is shown in Figure 1. The test stand consists of a platform normally connected to the three point hitch of the tractor on which a boom and its suspension are mounted. This platform is now connected to two hydraulic cylinders, such that a shaker is obtained, simulating the tractor behaviour at two points of the three point hitch. Because only horizontal vibrations are considered, the third connection point is omitted.

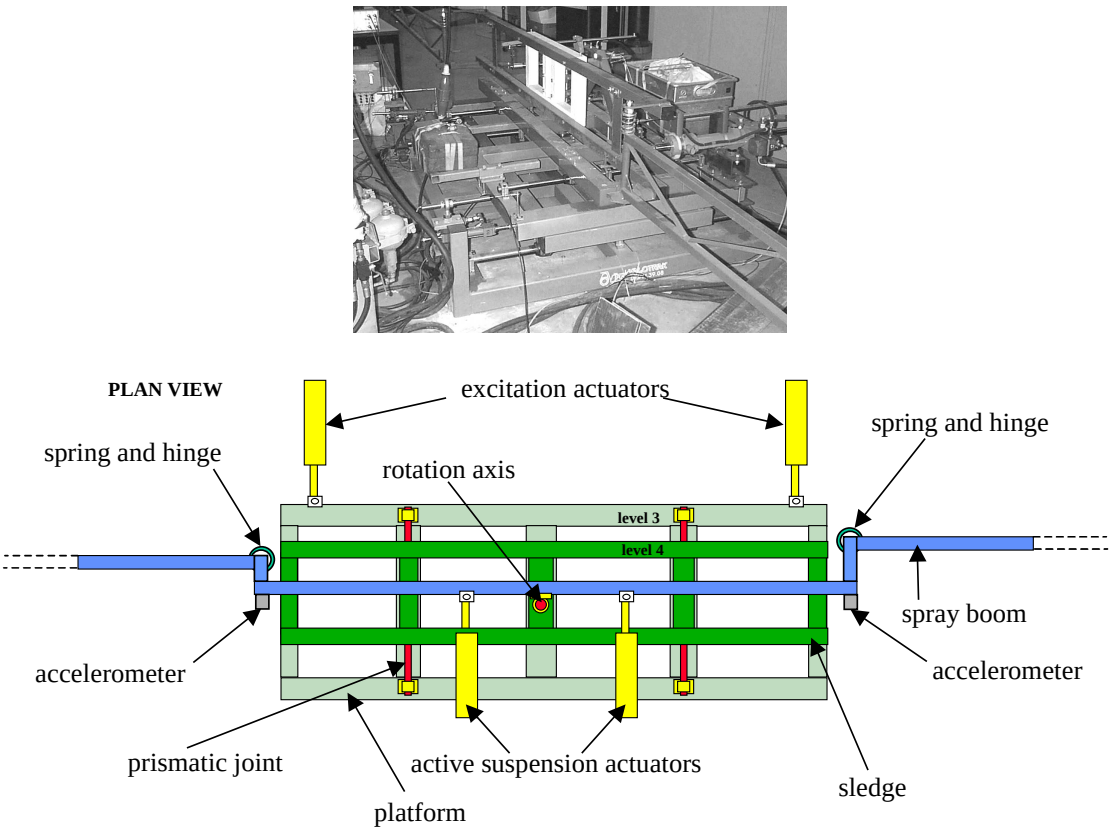

Figure 1 : Picture and sketch of the system.

To be able to isolate the boom from the tractor, the boom is given two degrees of freedom through a sledge and a rotation axis. Two control actuators, connected between the platform and the boom, serve to counteract the undesired vibrations. These hydraulic cylinders have an internal proportional position control loop. LVDT position sensors measure the relative position of the piston rod with respect to the housing of the cylinders. The proportional gains of the controllers are tuned such that the actuators perform a synchronised motion for identical input signals. Accelerometers with a bandwidth between 0 Hz and 150 Hz measure the transmitted vibrations on the boom. Consequently the final controller is

a cascade controller, consisting of two inner loop position controllers for each hydraulic cylinder and a master loop, calculating the control actions based on accelerometer measurements.

The boom itself is a commercial available 12 m Delvano spray boom which can be folded and unfolded in two hinges on each side of the boom. Springs connected in the hinges keep the boom in its unfolded configuration. The middle part of the boom can be considered as rigid. Flexibility's are mainly in the framework structures after the hinges and in the hinges. To make a vibrations isolator and in order to obtain large sensor signals, the accelerometers are placed at the ends of the rigid middle structure. By preventing the rigid middle structure to vibrate, also the boom tips will not be excited and together rigid body motions and flexible deformations are reduced.

3 Peculiarities of the system

From the previous it is clear that the system to be controlled is a MIMO system in which two control actuators need to counteract the vibrations generated by two excitation actuators by means of two accelerometers. Consequently the relation between the actuators and the accelerometers is as follows :

$$\begin{bmatrix} y_1 \\ y_2 \end{bmatrix} = \begin{bmatrix} G_{11}(s) & G_{12}(s) \\ G_{21}(s) & G_{22}(s) \end{bmatrix} \begin{bmatrix} u_1 \\ u_2 \end{bmatrix} + \begin{bmatrix} H_{11}(s) & H_{12}(s) \\ H_{21}(s) & H_{22}(s) \end{bmatrix} \begin{bmatrix} w_1 \\ w_2 \end{bmatrix} \qquad (1)$$

in which y_1, y_2 are the accelerometer signals, u_1,u_2 the control inputs, w_1, w_2 the excitation actuator (disturbance) inputs and $G_{11}(s)$, … and $H_{11}(s)$ the transfer functions, describing the dynamical relation between each control respectively each disturbance input and each output.

Experiments on the set-up reveal that by steering the control or excitation actuators in phase or in opposite phase, only translational respectively rotational modes can be excited. This implies that there exists 2 separate transfer functions : one describing the translations and the other describing the rotations. Therefore by changing from the physical available input (u_1, u_2, w_1, w_2) and output (y_1, y_2) coordinates to coordinates expressing purely translations and rotations, the transfer function matrices become diagonal :

$$\begin{bmatrix} y_t \\ y_r \end{bmatrix} = \begin{bmatrix} G_t(s) & 0 \\ 0 & G_r(s) \end{bmatrix} \begin{bmatrix} u_t \\ u_r \end{bmatrix} + \begin{bmatrix} H_t(s) & 0 \\ 0 & H_r(s) \end{bmatrix} \begin{bmatrix} w_t \\ w_r \end{bmatrix} \qquad (2)$$

where subscripts t and r stand for rotations and translations respectively. The straight forward link between (1) and (2) is given by :

$$\begin{bmatrix} G_{11}(s) & G_{12}(s) \\ G_{21}(s) & G_{22}(s) \end{bmatrix} = T_y^{-1} \begin{bmatrix} G_t(s) & 0 \\ 0 & G_r(s) \end{bmatrix} T_u \qquad (3)$$

$$\begin{bmatrix} H_{11}(s) & H_{12}(s) \\ H_{21}(s) & H_{22}(s) \end{bmatrix} = T_y^{-1} \begin{bmatrix} H_t(s) & 0 \\ 0 & H_r(s) \end{bmatrix} T_w \qquad (4)$$

in which T_u, T_w, T_y are the matrices to transform the coordinates from physical inputs to translational and rotational inputs for the control and excitation inputs and outputs respectively. Transfer function matrices satisfying (3) and (4) are called dyadic transfer function matrices (DTM) and allow to reduce MIMO controller design to n SISO designs in which n is the number of columns and rows in the

transfer function matrix (Owens, 1978). Optimality of a MIMO controller, obtained by performing n SISO designs, is proven when the transformation matrices in (3) and (4) are unitary (Hovd *et al.*, 1997). The transformation matrices in (3) and (4) reduce to the same unitary matrix, by scaling the rows of T_u and T_w and the columns of T_y and therefore (3) turns into :

$$\begin{bmatrix} G_{11}(s) & G_{12}(s) \\ G_{21}(s) & G_{22}(s) \end{bmatrix} = \begin{bmatrix} 1/\sqrt{2} & 1/\sqrt{2} \\ -1/\sqrt{2} & 1/\sqrt{2} \end{bmatrix}^T \begin{bmatrix} G_t(s) & 0 \\ 0 & G_r(s) \end{bmatrix} \begin{bmatrix} 1/\sqrt{2} & 1/\sqrt{2} \\ -1/\sqrt{2} & 1/\sqrt{2} \end{bmatrix} \tag{5}$$

The entries of $G_t(s)$, $G_r(s)$ are scaled versions of the entries in (3) but for ease of notation, no distinction has been made. The same can be done for equation (4). Remark that $G_t(s)$ and $G_r(s)$ coincide with the eigenvalues and the absolute values of $G_t(s)$ and $G_r(s)$ to the singular values of the system transfer function matrix. Strictly speaking, it is not necessary that the absolute values of $G_t(s)$ separately or $G_r(s)$ separately match with a certain singular value curve, because it may be possible that the absolute value of $G_t(s)$ in a certain frequency point is smaller then the absolute of $G_r(s)$ but that in another frequency point the opposite is true. Therefore $G_t(s)$ and $G_r(s)$ are rearranged singular value curves, having the physical interpretation of a motion, also equalling the eigenvalues of the system transfer function matrix. Hovd *et al.* (1997) considered also these rearranged singular value curves and proved that in case n SISO H^∞ controllers are designed, the resulting MIMO controller is super optimal. The term super optimal comes from the fact that in each SISO controller design step, a rearranged singular value curve is shaped to its optimal form, whereas in a single MIMO design step, only the maximum of all these curves is optimised i.e. the maximum singular value in strict sense. The result can intuitively understood from the fact that stability is determined by the eigenvalue curves of the system transfer function matrix and that performance is related to the amplification characteristics expressed through the singular values which are globally left unchanged. He also proved optimality for H^2 controllers but the optimality for μ designs can only be guaranteed for a certain class of block diagonal structures. This class has to do with the fact that it introduces uncertainty coupling between the rearranged singular values.

When n SISO designs are performed, the global MIMO controller takes the following structure and is called an SVD-controller (Singular Value Decomposition) :

$$\begin{bmatrix} 1/\sqrt{2} & 1/\sqrt{2} \\ -1/\sqrt{2} & 1/\sqrt{2} \end{bmatrix}^T \begin{bmatrix} K_t(s) & 0 \\ 0 & K_r(s) \end{bmatrix} \begin{bmatrix} 1/\sqrt{2} & 1/\sqrt{2} \\ -1/\sqrt{2} & 1/\sqrt{2} \end{bmatrix} \tag{6}$$

with $K_t(s)$ and $K_r(s)$ the calculated controllers in each SISO design step.

4 Modeling of the system

Based on input-output measurements, a black box model is identified for the transfer from the control inputs u_1, u_2 to the accelerometer signals y_1, y_2. This can be done by keeping the excitation actuators, generating the transmitted tractor vibrations, in their middle position. Because of the structure of the system transfer function (5), MIMO identification reduces to 2 SISO identifications. The transfer function describing the translations, $G_t(s)$ is determined from experiments in which the control actuators give the same inputs to the boom, whereas for the rotations $G_r(s)$, the actuators are steered also with the same inputs but in opposite phase. Actually, $G_t(s)$ and $G_r(s)$ can be determined through the same experiment, but to avoid correlation between the translational and the rotational part, two separate experiments are performed. For the calculation of the models, the measured inputs and

outputs are transformed to a purely translational and a rotational component through the unitary matrix :

$$\begin{bmatrix} 1/\sqrt{2} & 1/\sqrt{2} \\ -1/\sqrt{2} & 1/\sqrt{2} \end{bmatrix} \qquad (7)$$

which is also used in (5) and (6). For the translational and the rotational experiments, only the relevant components are retained i.e. only the translational component or only the rotational component.

During the experiments, all the excitation signals are applied periodically to the system to avoid leakage errors. When the system is in steady-state, 8 excitation periods are measured. The effect of noise is reduced by averaging over the 8 measurement periods.

Excitation signals are generated by a PC and are sent to the control actuators via a digital to analogue (D/A) converter. The measured accelerations are collected through an analogue to digital (A/D) converter in the same PC. The send out frequency of the D/A and A/D converter are selected 10 times the maximum frequency of interest i.e. 200 Hz which is a rule of thumb in sampled data experiments. Because only low frequent vibrations can cause large boom movements, a maximum frequency of 20 Hz is certainly sufficient. To avoid aliasing, an 8^{th} order Butterworth filter with a cut-off frequency of 20 Hz is employed. The effect of the filter is cancelled by using in the identification step inputs and outputs which are both measured and filtered.

A model for $G_t(s)$ and $G_r(s)$ is determined by performing black box frequency domain identification. As most of the H^∞ controller design theory and algorithms to calculate the optimal controller are founded on continuous models, the advantage of frequency domain identification is that it can provide directly a continuous model. Due to the continuous nature of the model, it is also easy to insert previous knowledge of the system based on physical properties in the proposed model structure. Here a non-linear least squares black box frequency domain identification is performed, involving the minimisation of the following cost function :

$$\hat{\Theta} = \arg\min_{\Theta} \left(\sum_{k=1}^{N} \left| FRF(j\omega_k) - \hat{P}(j\omega_k, \Theta) \right|^2 \right) \qquad (8)$$

in which :

$$\hat{P}(j\omega_k, \Theta) = \frac{B(j\omega_k, \Theta)}{A(j\omega_k, \Theta)} = \frac{\sum_{i=0}^{n_b} b_{n_b - i} (j\omega_k)^i}{(j\omega_k)^{n_a} + \sum_{i=0}^{n_a - 1} a_{n_a - i} (j\omega_k)^i} \qquad (9)$$

is a parametric estimate of the transfer function of the system, evaluated on the imaginary axis at frequency point $j\omega_k$. The parameters $b_{n_b - i}$ and $a_{n_a - i}$ are collected in the vector Θ which has to be determined. Indices n_a and n_b are the highest degree of the denominator and the numerator respectively. The initials FRF stand for frequency response function estimate and $\hat{P}(j\omega_k, \Theta)$ for a

model estimate of $G_t(s)$ or $G_r(s)$. An overview of frequency domain identification methods is given in (Pintelon *et al.*, 1994) and (Schoukens and Pintelon, 1991).

From previous studies (Kennes *et al.*, 1998) on the experimental arrangement, it has been found out that the boom and also the platform contain non-linearity's. This is also confirmed by experiments with different excitation signals which show after the collection of the data, differences in the calculated FRF's (Figure 2). A random sequence with a frequency band between 0 Hz and 20 Hz, a swept sine and two different multisines are used, each consisting of 4096 points. Especially for the translations, differences are visible at higher frequencies. The FRF calculated from measurements with a random excitation are noisier. Because of the random nature of the signal, some frequency lines are poorly excited resulting in a low signal to noise ratio. In order to capture as good as possible the global behaviour of the system in a linear model, the model is identified on the average of the different FRF's.

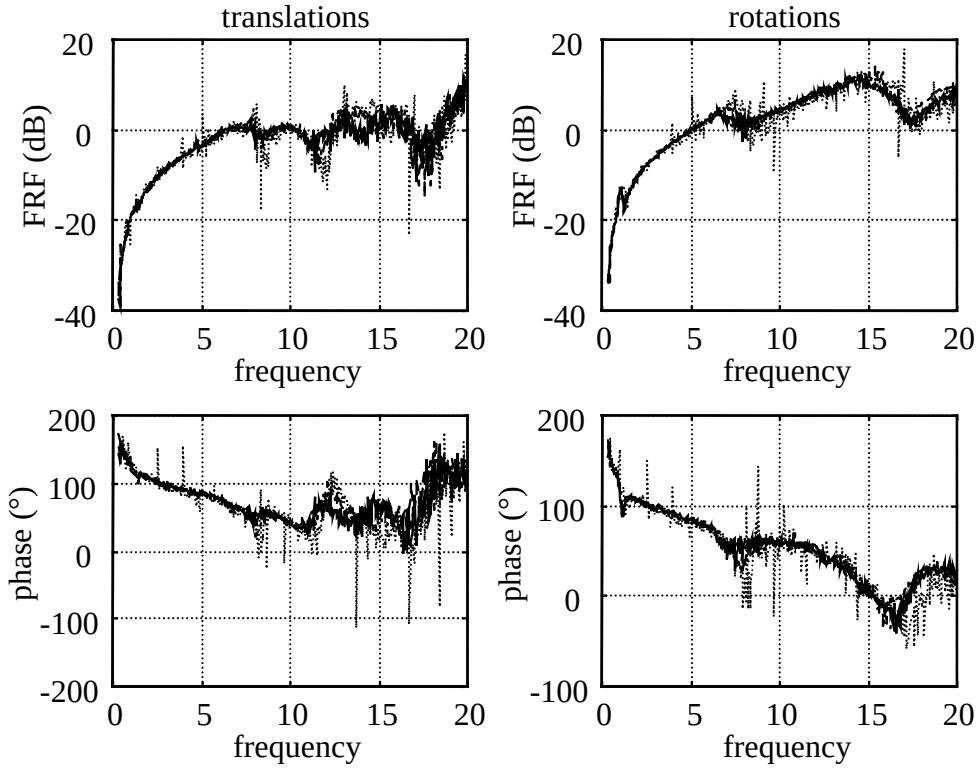

Figure 2 : Frequency response functions for different excitation inputs (dotted : random input, dashed : swept sine, dash-dot : multisine 1, solid line : multisine2)

Before starting the optimisation process in (8) a certain model structure of which the parameters are calculated must be proposed. The set of possible model structures can be reduced, when some previous knowledge is present. Because of the position feedback on the control actuators, they impose a position on the middle frame of the boom. As the middle frame is rigid and accelerometers measure the motions of this frame, a double differentiator should be incorporated in the model structure. The presence of a double differentiator is also visible in the FRF's of Figure 2. For the translations, a 6^{th} order model with numerator and denominator of the same degree, seems to trade off the best between model complexity and accuracy. In the case of rotations, a 4^{th} order model with numerator and denominator of the same degree is selected. The identification results are depicted in Figure 3

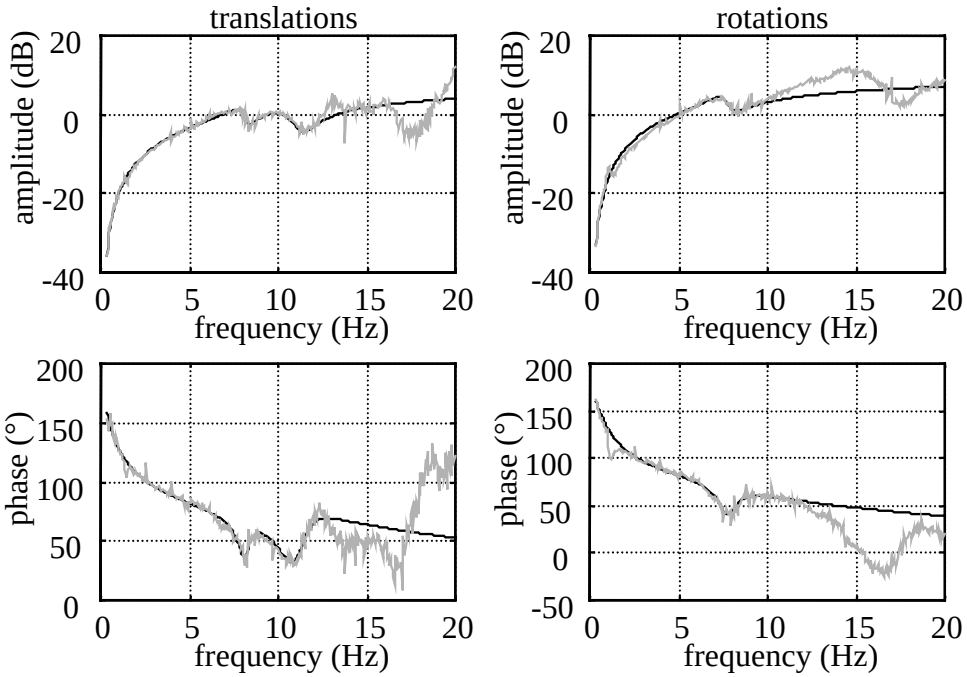

Figure 3 : Frequency domain identification results (black line : model, grey line : average FRF).

5 Controller design

The H^{∞} methodology is applied to design the controller. An advantage of this method is that shaping of a certain transfer function can easily performed and that both robustness and performance can be taken into account. As the control cost function after optimisation is all pass (Chiang and Safonov, 1992a), by inserting weights in the control cost function, the selected transfer between certain signals can be put in the desired form. As mentioned earlier, the design of a controller for the translations and the rotations is performed separately.

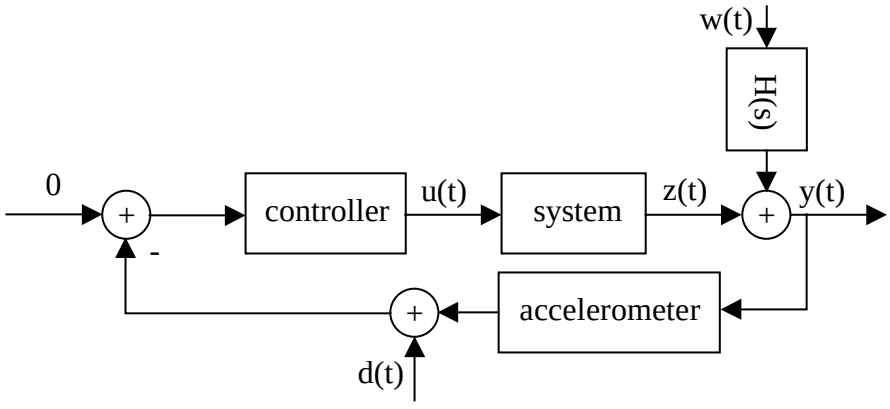

Figure 4 : Control problem design scheme.

The control problem is depicted in Figure 4. When an input is sent to the control actuators, the boom starts to move with respect to the platform. The absolute acceleration y(t) is constituted of the relative accelerations z(t) induced by the control actuators and the accelerations induced by the tractor

vibrations w(t). Accelerometers measure y(t) and because of sensor imperfections, noise d(t) is added. It turns out that the most important component in d(t) is low frequent accelerometer drift, induced by the amplifiers. Because of (3) and (4), the scheme in Figure 4 can be applied separately for the translations and the rotations.

The design objective is to reduce the influence of the tractor vibrations w(t) on the spray boom motions, implying a sensitivity S(s) minimisation. Low frequent motions of the tractor like accelerations and turning over the field should be followed by the boom, whereas high frequent vibrations don't cause large boom motions and consequently don't lead to a non-uniform spray pattern. Therefore it is only necessary to reduce the transmitted tractor vibrations in a narrow frequency band. This can be achieved by shaping the sensitivity to a band stop filter. In an H^{∞} framework, shaping is accomplished by searching for a controller such that :

$$\left\| \alpha W_1(s) S(s) \right\|_{\infty} < 1 \qquad (10)$$

is fulfilled, where α is a tuning constant and $W_1(s)$ a factor amplifying in the desired frequency band. By raising α, the steepness of the band stop filter is increased, which can be done until no controller exists anymore. At this point the optimal controller is found. $W_1(s)$ is displayed in Figure 5 and is constructed by cascading two transfer functions :

$$\frac{s^2 + 2\zeta_n \omega_n s + \omega_n^2}{s^2 + 2\zeta_d \omega_n s + \omega_n^2} \qquad (11)$$

By tuning ζ_n and ζ_d the height of the peaks at ω_n is modified. To have a good vibration suppression, the first peak is put at the first eigenfrequency of the boom which is for the translations and the rotations as well at 1.2 Hz. As high frequency vibrations don't cause any harm to the spray pattern, the second peak is selected at 3 Hz.

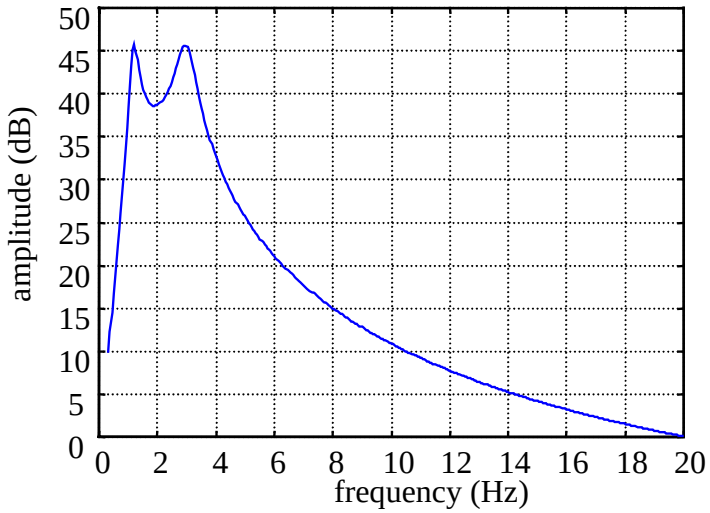

Figure 5 : Amplitude plot of the sensitivity design weight $W_1(s)$

Another objective is to avoid the propagation of the accelerometer drift to the output, which involves also shaping of the complementary sensitivity T(s). This could be performed by optimising a similar cost function as (10) but, S(s) replaced by T(s) and a weight amplifying at low frequencies. However,

practical implemented controllers were not that effective against accelerometer drift. Tighter weights on T(s) turned out to be too conflicting with the specification of (10). Therefore the accelerometer signals are passed through a high pass filter (s/(s+1)), before entering the controller.
To guarantee a stable controller on the real system, model imperfections must be taken into account. Here the model deviations Δ_M are considered multiplicative i.e. :

$$P_0(s) = \hat{P}(s)(1 + \Delta_M(s)) \qquad (12)$$

in which $P_0(s)$ is the behaviour of the real system and $\hat{P}(s)$ the identified model for either the translations or the rotations. The transfer function seen by Δ_M is the complementary sensitivity T(s). Let

$$\Delta_M(s) = W_2(s)\Delta_{M_0} \qquad (13)$$

and $\left\|\Delta_{M_0}\right\|_\infty \le 1$, then, as has been shown by (Doyle *et al.*, 1992), the system is stable iff the following condition is met :

$$\left\|W_2(s)T(s)\right\|_\infty < 1 \qquad (14)$$

Combining the design requirements (10) and (14), results in the following condition :

$$\left\| \begin{matrix} \alpha W_1(s)S(s) \\ W_2(s)T(s) \end{matrix} \right\|_\infty < 1 \qquad (15)$$

To obtain a non-conservative result, (15) should be optimised by μ synthesis. However, a bad estimate of the size of the uncertainties as a function of frequency i.e. improper choice of $W_2(s)$ can also introduce too much conservativeness. Additionally, the complexity of $W_2(s)$ enlarges the dimensions of the controller. Therefore an ad hoc approach is followed. As a starting point, $W_2(s)$ is selected constant and gamma-iteration is performed on (15). After controller design, the robustness is checked. From (12), a reasonable estimate of the multiplicative uncertainty Δ_M can be calculated, by replacing the unknown, but real life system $P_0(s)$ by its FRF :

$$\Delta_M(j\omega) = \frac{FRF(j\omega)}{\hat{P}(j\omega)} - 1 \qquad (16)$$

To take into account as much as possible the non-linearity's of the system, a multiplicative uncertainty curve $\Delta_M(j\omega)$ is calculated for each FRF, computed from measurements, collected when one of the four excitations signals is applied. From the small gain theorem (Skogestad and Postlethwaite, 1996), it is easily deduced that the closed loop system is stable if :

$$\left\|\Delta_M(s)T(s)\right\|_\infty < 1 \qquad (17)$$

is satisfied, or

$$|\Delta_M(j\omega)| < \frac{1}{|T(j\omega)|} \qquad (18)$$

, holds for all frequencies. (18) implies that the absolute value of the inverse of the complementary sensitivity can serve as a robustness bound. If a multiplicative uncertainty curve $\Delta_M(j\omega)$ crosses the robustness bound, the constant weight is increased. This operation is repeated until all curves are below the robustness bound. When no sufficient performance is attained, dynamics can be incorporated in $W_2(s)$. The robustness tests for the final controller for the translations and the rotations are depicted in Figure 6 and Figure 7. A constant weight for both the translations and the rotations rendered a sufficient performance (Figure 8). In case of the random signal, still some spikes are crossing the robustness bound. They are not taken into account because, it is expected that they come from noise, inherently connected to the random excitation, and not from model deviations.

It should be noted that during controller design the high pass filters, to remove the drift of the accelerometers, were not taken into account, giving rise to a small amplification at low frequencies in the sensitivity function Figure 8. Incorporating the high pass filters in the controller design, cancels their effect, resulting again in drifting of the actuators. However the small amplification can be reduced, by lowering the pole of the high pass filter.

During the H^{∞} control synthesis, it turned out that the problem formulation was ill-conditioned, due to $j\omega$-axis zeros introduced by the double differentiators. This problem is solved by applying the bilinear pole shifting transform technique (Chiang and Safonov, 1992b). Here the imaginary axis is shifted 0.1 units to the right.

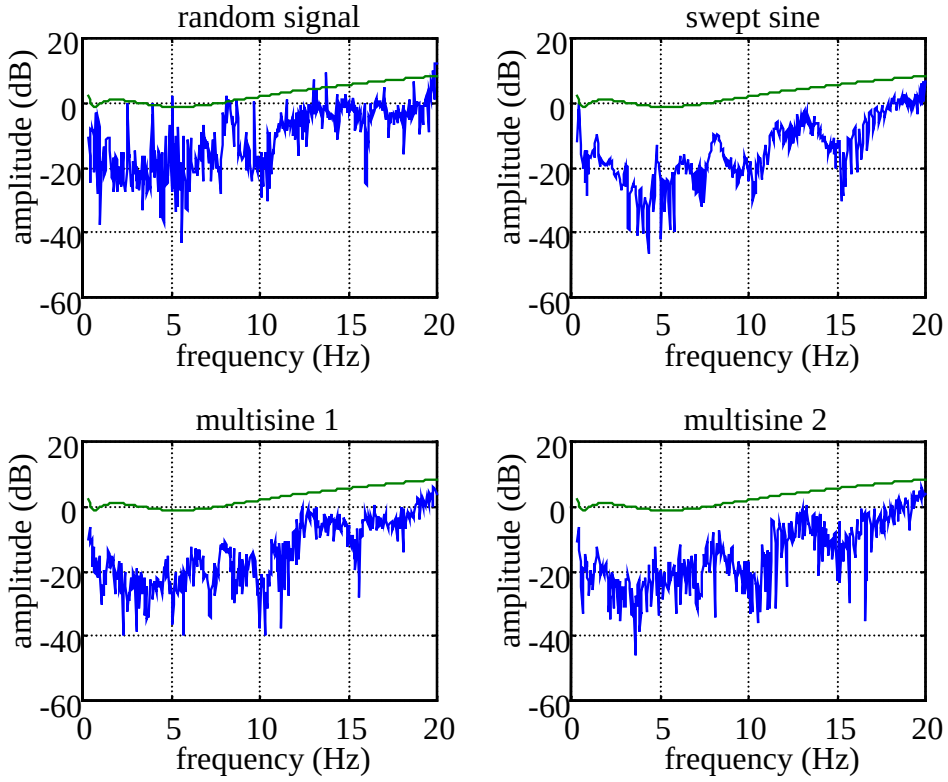

Figure 6 : Robustness test for the final controller for the translations.

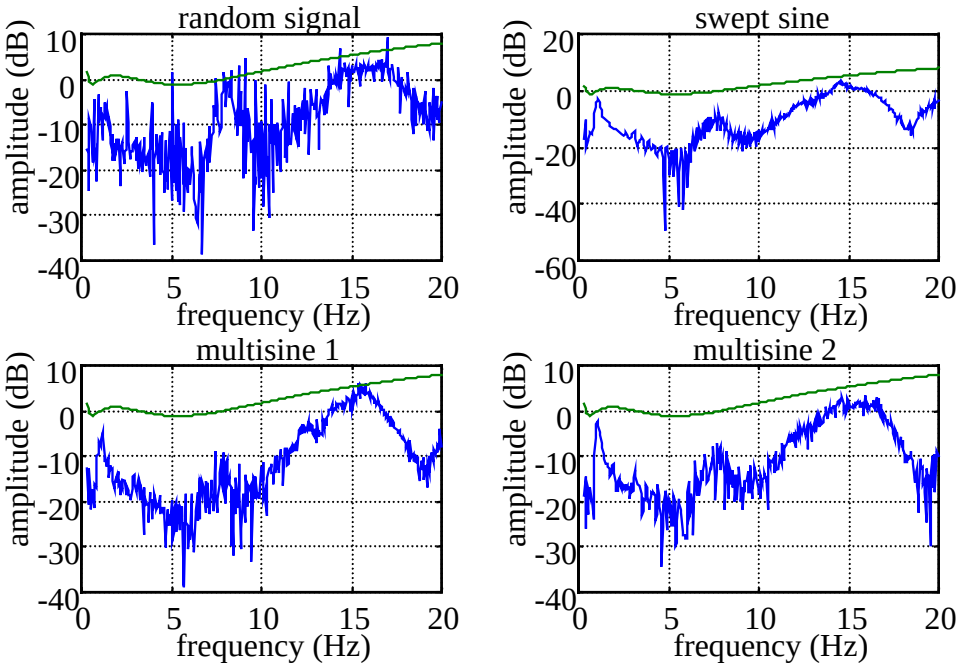

Figure 7 : Robustness test for the final controller for the rotations.

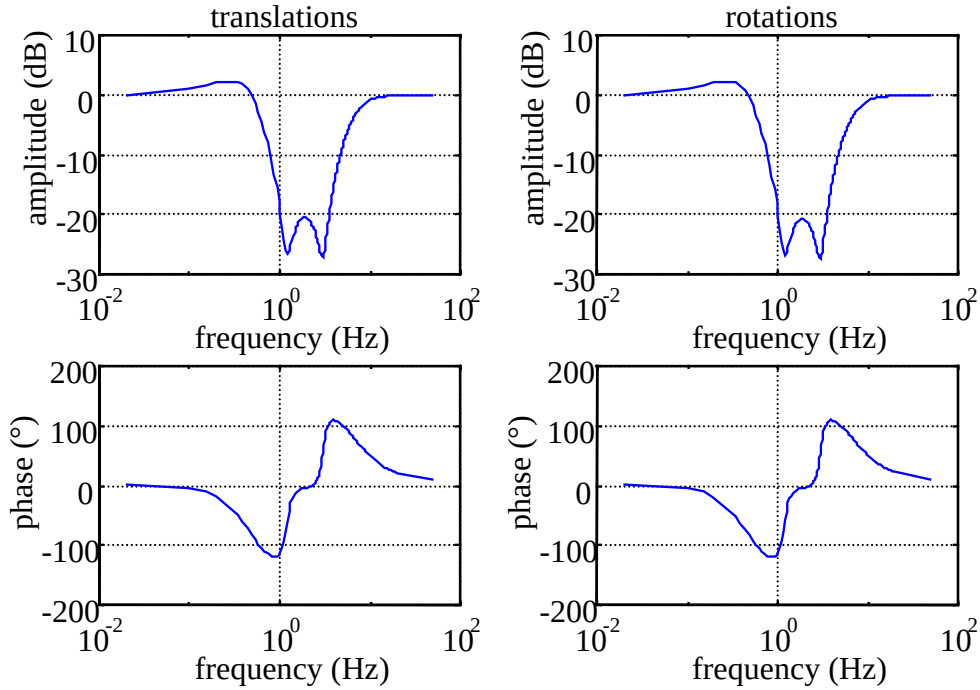

Figure 8 : Designed performance of the controllers (sensitivity function).

6 Controller validation.

The final controller (6) is implemented on the experimental arrangement. Figure 9 shows a measured boom tip motion when a signal near the eigenfrequency of the boom is applied. An attenuation of boom movements of more than 10 is achieved.

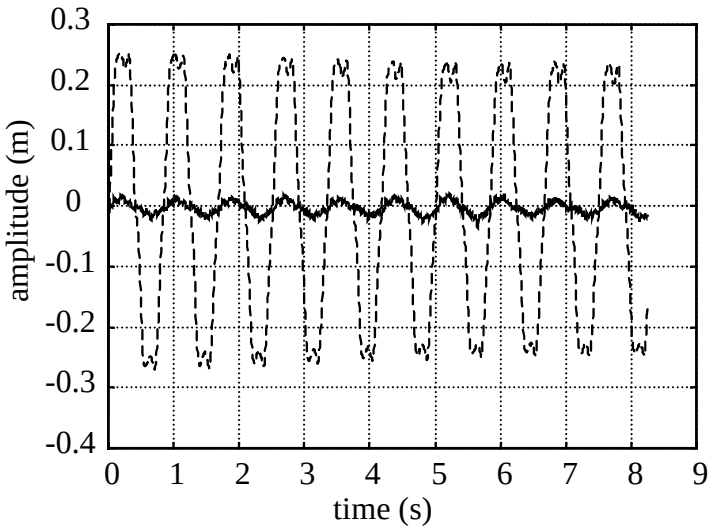

Figure 9 : Boom tip motion with (solid line) and without controller (dashed line).

Robustness is checked by adding mass to the sledge. Even with a weight of 150 kg on it, which is approximately 2 times the weight of the sledge-boom assembly, the controller remained stable and still a good performance is achieved. Also a bucket filled with water, connected at a boom tip, lowering the eigenfrequency from 1.2 Hz to 0.7 Hz, couldn't make the controller unstable. In this case, the performance is lost.

7 Conclusions.

By averaging the FRF's, calculated from measurements from different excitation signals, black box frequency domain identification techniques deliver continuous models covering the global linear system behaviour.

A MIMO controller, turning the attenuation characteristics of an active suspension to a band stop filter, is designed. This is performed by two H^{∞} SISO designs, rendering a global MIMO super optimal controller. Separate high pass filters, avoid the propagation of accelerometer drift to the output. An ad hoc approach, based on the calculation of an estimate of the multiplicative uncertainty and the small gain theorem, is followed to take into account model deviations.

Experiments on a commercial available spray boom show a good performance and a large robustness of the controller. Flexible deformations as well aw rigid body motions of the boom are attenuated.

8 References.

Chiang R. Y., Safonov M. G. (1992a) *Robust control toolbox user 's guide.* The Math Works Inc.

Chiang R. Y. and Safonov M. G. (1992b) "H^{∞} Synthesis using a bilinear pole shifting transform," *Journal of Guidance, Control and Dynamics,* **15**, No. 5, pp. 1111-1117.

Doyle J. C., Francis B. A., Tannenbaum A. R. (1992) *Feedback control theory*. Macmillan Publishing Company.

Hovd M., Braatz R. D., Skogestad (1997), "SVD controllers for H^2-, H^{∞}- and μ- optimal control," *Automatica,* **33**, No. 3, pp. 433-439.

Kennes P., Vermeulen K., Ramon H. (1998) "Evaluation of a non-linear finite element model to simulate vibrations of a small size sprayer boom," *Preprints of the proceedings of the 1st IFAC Workshop on Conrol Applications and Ergonomics in Agriculture,* Athens, Greece, June, pp. 309-313.

Langenakens J. J., Ramon H., De Baerdemaeker J. (1995) "A model for measuring the effect of tire pressure and driving speed on the horizontal sprayer boom movements and spray patterns," *Transactions of the ASAE,* **38,** No. 1, pp. 65-72.

Owens D. H. (1978), *Feedback and multivariable systems*, PeterPeregrinus LTD.

Pintelon R., Guillaume P., Rolain Y., Schoukens J. and Van Hamme H. (1994) "Parametric identification of transfer functions in the frequency domain – A survey," *IEEE Trans. Automat. Contr.,* **39**, No. 11, pp. 2245-2260.

Ramon H. (1993) *A design procedure for modern control algorithms on agricultural machinery applied to active vibration control of a spray boom.* PhD Dissertation Department of Agricultural Engineering. K.U. Leuven, Belgium.

Ramon H., De Baerdemaeker J. (1996) "Design of a cascade controller for a flexible spray boom," *Mechanical Systems and Signal Processing,* **10**(2), pp. 197-210.

Ramon H., De Baerdemaeker J. (1997) "Spray boom motions and spray distribution: part 2, Experimental validation of the mathematical relation and simulation results," *J. agric Engng. Res.* **66**, pp. 23-29.

Schoukens J. and Pintelon R. (1991) *Identification of Linear Systems, A practical guide to Accurate Modeling.* New York Pergamon Press.

Skogestad S., Postlethwaite I. (1996) *Multivariable feedback control, Analysis and Design.* John Wiley & Sons, Chichester, New York, Brisbane, Toronto, Singapore.

Speelman L., Jansen J.W. (1974) "The effect of spray boom movements on the liquid distribution of field crop sprayers," *J. agric. Engng. Res.*, **19**, pp. 117-129.